Adv. Polar Upper Atmos. Res., **16**, 157–172, 2002

Polar Patrol Balloon experiment in Antarctica during 2002–2003

Akira Kadokura[1], Hisao Yamagishi[1], Natsuo Sato[1], Masaki Ejiri[1], Haruto Hirosawa[2], Takamasa Yamagami[2], Shoji Torii[3], Fumio Tohyama[4], Michio Nakagawa[5], Toshimi Okada[6] and Edgar A. Bering[7]

[1]*National Institute of Polar Research, Kaga 1-chome, Itabashi-ku, Tokyo 173-8515*
[2]*The Institute of Space and Astronautical Science, Sagamihara, Kanagawa 229-8510*
[3]*Institute of Physics, Kanagawa University, Kanagawa-ku, Yokohama 221-8686*
[4]*Faculty of Engineering, Tokai University, Hiratsuka, Kanagawa 259-1292*
[5]*Faculty of Science, Osaka City University, Sumiyoshi-ku, Osaka 558-8585*
[6]*Faculty of Engineering, Toyama Prefectural University, Toyama 939-0398*
[7]*Physics Department, University of Houston, Houston, Texas, 77204-5506, U.S.A.*

Abstract: The first scientific campaign of the Polar Patrol Balloon (PPB) experiment (1st-PPB) was performed at Syowa Station in Antarctica during 1990–1991 and 1992–1993. Based on the fruitful results of the 1st-PPB experiment, the next campaign (2nd-PPB) will be carried out in the austral summer of 2002–2003. This paper summarizes the 2nd-PPB experiment. Four balloons in total will be launched to make astrophysics observations (1 balloon) and upper atmosphere physics observations (3 balloons). The first payload will carry a very sophisticated instrument that will observe primary cosmic-ray electrons in the energy range of 10 GeV–1 TeV. The payloads of the latter 3 flights are identical to each other. They will be launched in as rapid a succession as weather conditions permit to form a cluster of balloons during their flights. Such a "Balloon Cluster" is suitable for observing the temporal evolution and spatial distribution of various phenomena in the various magnetospheric and ionospheric regions and their boundaries that the balloons will traverse during their circumpolar trajectory. The expected flight duration of each balloon is 20 days. Observation data will be obtained mainly by a satellite communication system with a much higher temporal resolution than that used in the 1st-PPB experiment.

1. Introduction

The "Polar Patrol Balloon (PPB)" experiment is a project involving long-term observations in the Antarctica using stratospheric zero-pressure balloons and the stable circumpolar easterly wind that occurs during austral summer. A feasibility study and the development of the balloon technology for the PPB started in 1984 as a 5-year project of the upper atmosphere physics group at the National Institute of Polar Research (NIPR) in collaboration with the Institute of Space and Astronautical Science (ISAS) and nationwide scientists (Nagata *et al.*, 1985; Nishimura *et al.*, 1985). Two and one test flights of the PPB were carried out in 1987 and 1990 by the 28th and 30th Japanese Antarctic Research Expeditions (JARE), respectively, at Syowa Station in Antarctica. These test flights

confirmed the reliability of the predicted long-duration circumpolar trajectory and the effectiveness of the balloon technology for the PPB, including the flight altitude control (auto-ballasting) system, and the ARGOS satellite communication system (Kadokura *et al.*, 1991; Kadokura, 1995; Ejiri *et al.*, 1993; Yamanaka *et al.*, 1988). After these preparatory phases, the first scientific campaign of the PPB (1st-PPB) was performed during 1990–1991 and 1992–1993 by JARE-32 and JARE-34, respectively (Fujii *et al.*, 1989; Ejiri *et al.*, 1995; Nishimura *et al.*, 1994). A total 6 balloons (3 balloons per period) were launched in the 1st-PPB to perform observations of the total force of the geomagnetic field (PPB-1), ionospheric and magnetospheric phenomena (PPB-2, 4, 5), atmospheric ozone and aerosol (PPB-3), and cosmic rays and auroral X-rays (PPB-6), respectively. A summary of the 1st-PPB experiment is given in Table 1, and the trajectories of the 6 balloons are shown in Fig. 1. Observation data were obtained via the ARGOS system when the balloons exited the receiving range of Syowa Station. Twenty and forty ID numbers were assigned to one ARGOS transmitter to transfer the data obtained with a sampling rate of 16 and 32 bytes/30 s in the 1990–1991 and 1992–1993 experiments, respectively. The details of the Multi-ID ARGOS transmitter system was described by Fujii *et al.* (1992). A geomagnetic anomaly arising from the earth's crust around Antarctica was thoroughly investigated using total force observations performed with a proton magnetometer onboard PPB-1, -2, -4 and -5 (Tohyama *et al.*, 1993). Magnetospheric phenomena were observed using the instruments onboard PPB-2, -4, -5 and -6 (Ebihara *et al.*, 1996; Hirasima *et al.*, 1999). Flight PPB-6 was particularly successful, allowing a thorough study of auroral X-ray phenomena (Kodama *et al.*, 1995; Suzuki, 1996). Cosmic-ray protons were also observed during the PPB-6 flight (Yamagami *et al.*, 1994). Observations of the ozone and aerosols in the Antarctic ozone hole were successfully performed by PPB-3 for the first time (Kanzawa and Kondo, 1991; Kanzawa *et al.*, 1994; Hayashi *et al.*, 1994). Despite such fruitful scientific

Table 1. An experimental summary of the 1st-PPB campaign.

PPB no	launching date	flight duration (days)	balloon volume (x 10^3 m^3)	payload weight (kg)	ballast weight (kg)	total weight (kg)	control altitude (km)	sampling rate	observation item
1	Dec. 25, 1990	38	25	114.0	152	373.5	28	16byte /30sec	total-B
2	Jan. 05, 1991	30	32	191.5	152	471.0	28	16byte /30sec	total-B, vector E-field aurora X-ray
3	Sep. 23, 1991	6	5	161.8	145	370.3	18	32byte /2min	ozone, aerosol
4	Dec. 26, 1992	9	39.7	189.0	150	487.8	28	32byte /30sec	total-B, vector B vector E, aurora X-ray
5	Dec. 30, 1992	43	39.7	186.5	150	483.5	28	32byte /30sec	total-B, vector B vector E, aurora X-ray
6	Jan. 05, 1993	27	59.5	95.0	150	434.2	30	32byte /30sec	cosmic ray (X-ray, proton)

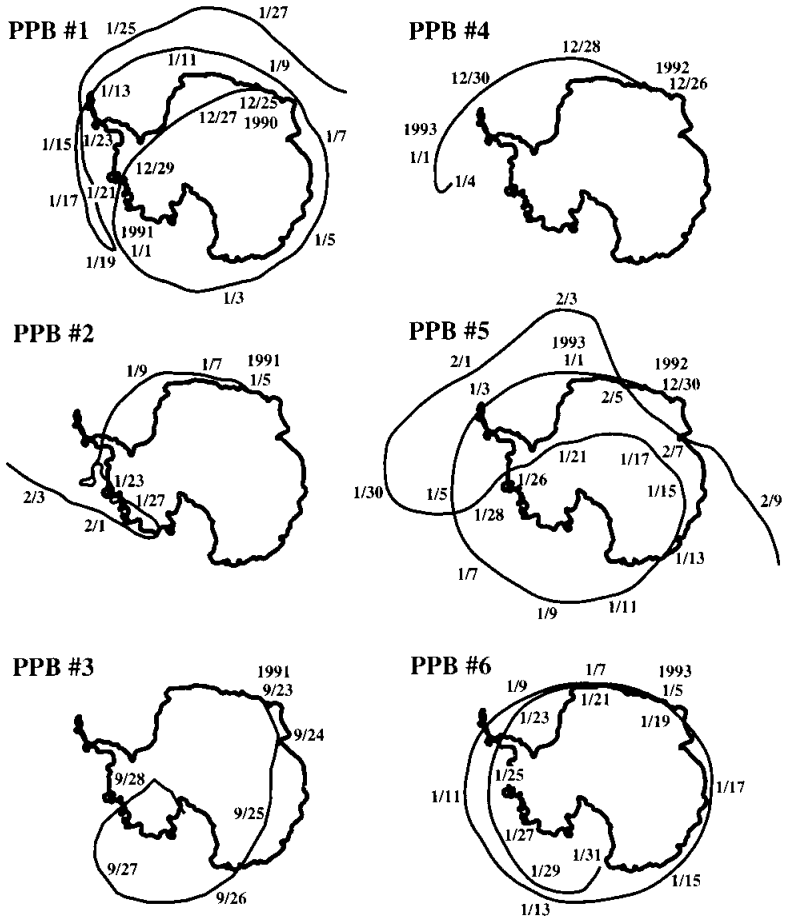

Fig. 1. Trajectories of the 6 balloons in the 1st-PPB campaign.

and balloon technological results in the 1st-PPB campaign, several objectives were not accomplished in the campaign, and the need for future experiments arose. The payload and balloon configurations of PPB-4 and PPB-5 were identical to each other to enable simultaneous observations at different local times. However, this objective was not fully accomplished because of failures in the altitude control systems of both balloons. Furthermore, the limited data acquisition rate of the Multi-ID ARGOS system was not sufficient for the observation of higher frequency phenomena, such as Pc3 or Pi2 pulsations, or for observations by more sophisticated instruments that required a larger amount of data to be transmitted. Scientific discussions for a future PPB experiment, based on the results of the 1st-PPB, began in 1995. Several workshops for that purpose were held at NIPR in 1995, 1997, and 1999. Eventually, the next PPB project (2nd-PPB) was scheduled as a 3-year project to be performed during 2000-2003. In the following sections, the details of the 2nd-PPB project will be introduced.

2. Overview of the 2nd-PPB project

The 3-year project will be conducted as follows: fabrication of the scientific payload for astrophysics observations in the 1st fiscal year (April 2000–March 2001), fabrication of the scientific payload for geophysics observations in the 2nd fiscal year (April 2001–March 2002), and integration of the total systems for each observation, and launching the payloads at Syowa Station in Antarctica in the 3rd fiscal year (April 2002–March 2003).

The campaign in Antarctica will be performed during late December 2002 to January 2003 by the 44th Japanese Antarctic Research Expedition (JARE-44). The primary launching window at Syowa Station is scheduled for the period from late December 2002 to early January 2003, mainly because of the requirements for a perfect westward circumpolar trajectory. After that period, the wind direction in the stratosphere gradually changes

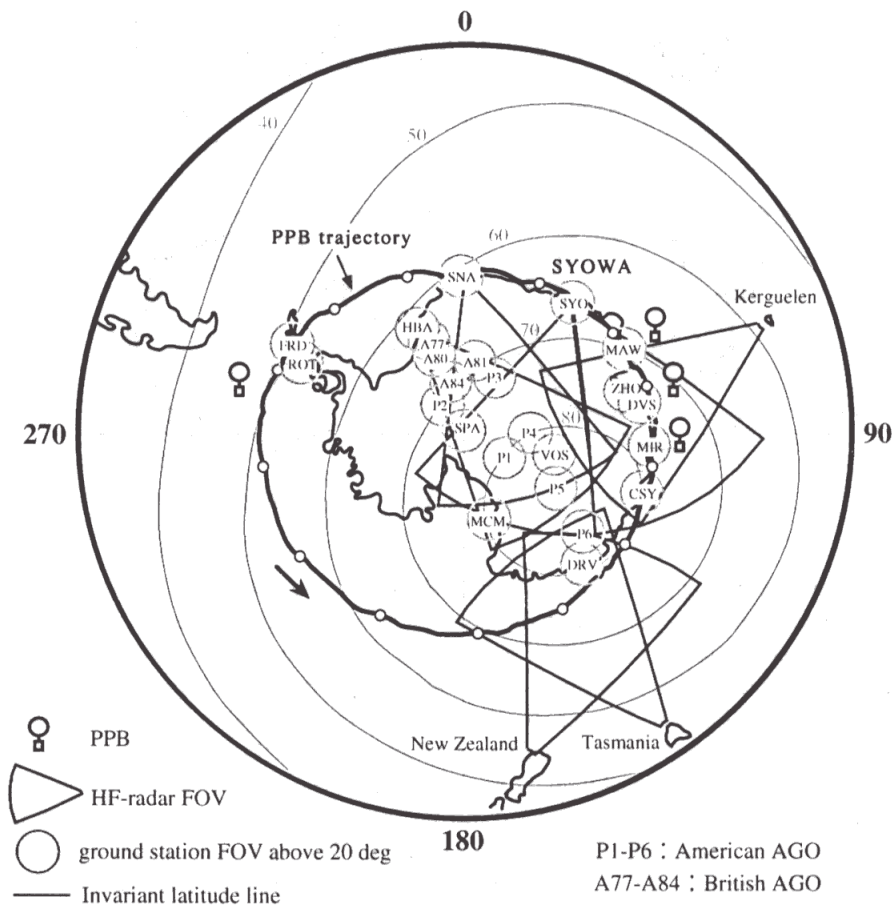

Fig. 2. Expected PPB trajectory. The contour of the equi-invariant latitude is shown by the gray curve. The location of ground stations, their FOVs above 20° elevation projected at an altitude of 120 km, and the FOVs of the HF-radars in the SuperDARN network are also shown.

from easterly to westerly. One 100000 m^3 zero-pressure balloon (B100) and three 50000 m^3 balloons (B50) will be launched during this period to perform astrophysical and geophysical observations, respectively. The flight altitudes will be controlled to within 35-40 km and 30-35 km for the astrophysical and geophysical observations, respectively, by the auto-ballasting system. The expected life time of each balloon is more than 20 days. The expected trajectory of the balloons is shown in Fig. 2. After their launch from Syowa Station, they will drift westward almost along the equi-geographic latitude line between $-60°$ and $-70°$ around the Antarctica with a circumpolar period of about 2 weeks. Since the geomagnetic dipole axis is tilted from the rotation axis of the earth, they will traverse a large geomagnetic latitudinal range between 50° and 80° invariant latitude (ILAT), shown by the gray-encircled contour in Fig. 2. The location of the ground stations, their field of views (FOVs) above 20° elevation projected at an altitude of 120 km, and the FOVs of the HF-radars in the SuperDARN network (Greenwald *et al.*, 1995) are also shown in Fig. 2. The balloons are expected to float within the FOVs of several ground stations and HF-radars during their circumpolar trajectory. Data will be downlinked via 64 kbps telemetry to several ground stations, including Syowa Station, and via a satellite data link system the Iridium satellite phone system, in which maximum transfer rate is 10 kbps. This transfer rate is about 2 orders of magnitude higher than the Multi-ID ARGOS system used in the 1st-PPB campaign. Accurate time and balloon positions will be obtained using GPS (Global Positioning System). Some basic house-keeping data, including the GPS data, will be obtained via the ARGOS satellite system.

The scientific payload for the astrophysical observations is an instrument for observing the primary cosmic-ray electrons in the energy range of 10 GeV to 1 TeV; this instrument has been named as PPB-BETS (Balloon-borne Electron Telescope with Scintillating Fibers for the PPB experiment). The instrumentation and scientific purpose of the BETS has been briefly described by Torii *et al.* (1999, 2000). Five instruments will be installed in the balloon payloads for the geophysical observations: an EMW (electromagnetic wave detector) to observe electromagnetic waves in the ULF to LF band range, an EFD (electric field detector) to observe the vector electric field, an MGF (magnetic field detector) to observe the vector geomagnetic field, an AXI (auroral X-ray imager) to observe auroral X-ray emissions, and a TEC (total electron content) to observe the total electron content of the ionosphere. The flight configurations for the astrophysical and geophysical observations are shown in Fig. 3a and 3b, respectively. The estimated payload weight, total ballast weight, total weight, and total lift with 11% of free lift for the astrophysical and geophysical observations are 500, 230, 730, and 810 kg and 340, 160, 500, and 555 kg, respectively. Electric power for the instruments is mainly supplied by a solar battery system. Five solar panel units are installed on each surface of a gondola. The maximum power output from one unit is 45 W, so each surface supplies 225 W. Each balloon has a parachute. If the balloon moves back within the FOV of Syowa Station after the circumpolar trajectory, the payload will be cut-down by a command from the ground and the recovery of the payload will be attempted. For the geophysical observations, two loop antennae for the EMW are set around the balloon surface orthogonal to each other, and the received signals are processed by the EMW main instrument in the sub-gondola. The sub-gondola consists of the EMW instrument and a reel-down. Since the EFD must avoid electric interference from charges on the balloon surface, the main gondola will be

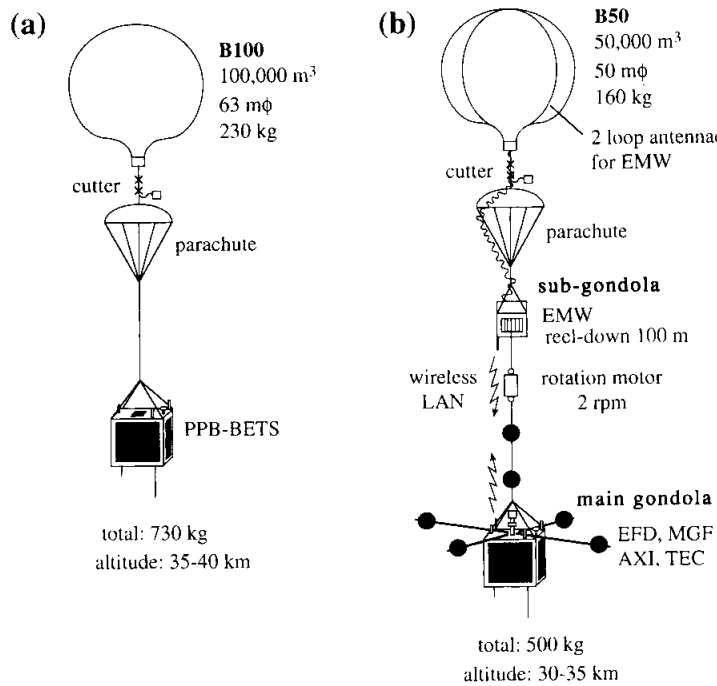

Fig. 3. Flight configurations for (a) astrophysical and (b) geophysical observations.

located 100 m below the sub-gondola. The EMW data processed in the sub-gondola is transmitted to the main gondola 100 m below via an RF modem. For the observational requirements of the EFD and MGF, a motor will be used to rotate the main gondola at a steady rate of 2 rpm. In the following sections, further details of the scientific instruments and scientific purposes of each type of observation will be described.

3. Astrophysical observations

Long-term observations by PPB are very useful for observing high-energy primary cosmic-ray electrons because the flux of these electrons is generally very small. The number of electrons expected to be observed during the 20-day PPB observation period is shown in Table 2. The statistical confidence of these observations should be increased by about 100 times, compared with that of usual experiments that last for less than one day. The life time of cosmic-ray electrons in the Galaxy is very short because they rapidly lose their energy through synchrotron and inverse Compton processes as they travel. The number of electron sources whose electrons reach Earth decreases as the energy of the electrons increases; SNRs (supernova remnants) and pulsars are known candidates for high-energy electrons sources, and the expected energy spectrum can be predicted by assuming the diffusion parameters. Table 3, taken from Torii *et al.* (1999), lists such candidates, and Fig. 4 shows the expected energy spectrum (black lines) and observed values in previous experiments (symbols). The expected observation range and values of

Table 2. Expected number of cosmic-ray electrons in the 20-days PPB observation.

Energy	> 10 GeV	> 100 GeV	> 1000 GeV
electron number	1.1×10^5	5.6×10^2	3

Table 3. List of SNRs and pulsars as candidaters of nearby electrons sources (after Torii et al., 1999).

SNR	Pulsar	Distance (kpc)	Age (yr)	Emax (TeV)
SN 185		0.95	1.8×10^3	130
S 147		0.8	4.6×10^3	50
G 65.3+5.7		0.8	2.0×10^4	12
Cygnus Loop		0.77	2.0×10^4	12
Vela	B 0833-45	0.5	$2\text{-}3 \times 10^4$	8-12
Monogem		0.3	1.0×10^5	2.3
Loop I		0.17	2.0×10^5	1.2
Geminga	IE 0630-178	0.3	3.4×10^5	0.7

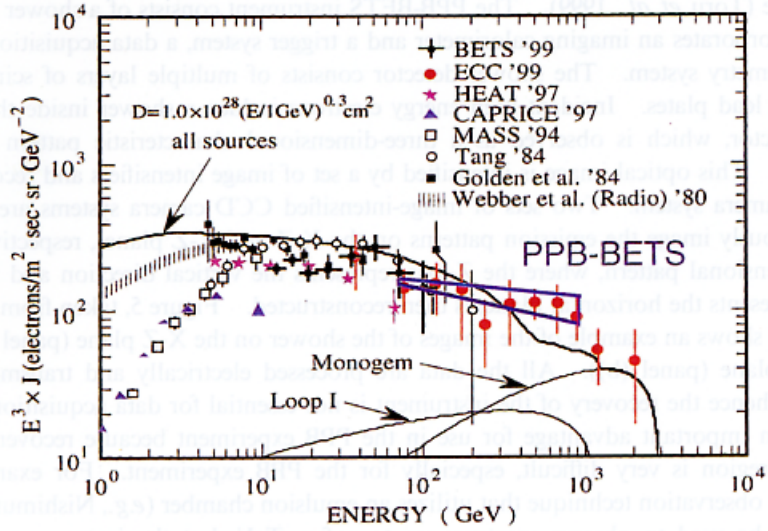

Fig. 4. Energy spectrum of the high-energy, cosmic-ray electrons. The expected energy spectrum (black lines) and the expected observation range and values of the PPB-BETS (blue line) are shown with the observed values obtained in previous experiments (symbols).

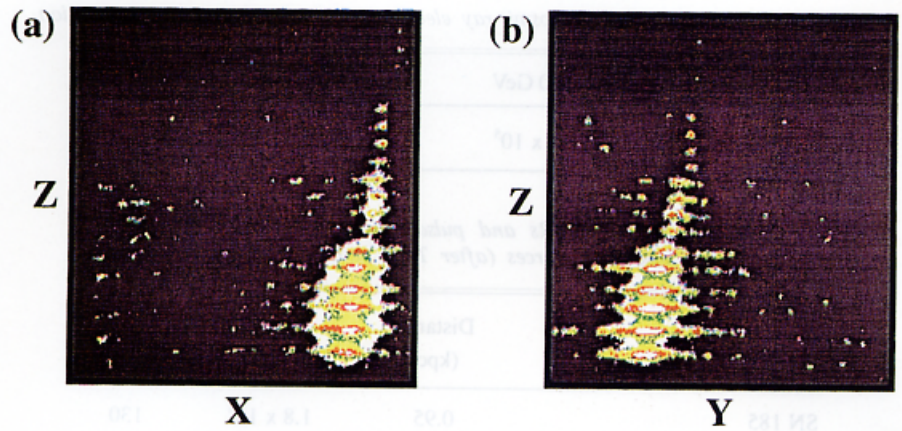

Fig. 5. CCD images of a cosmic-ray electron shower, observed by the BETS, on the X-Z plane (a) and the Y-Z plane (b) (after Torii et al., 2000).

the PPB-BETS is also shown as a thick, straight blue line in Fig. 4. Observations of the precise energy spectrum using the PPB-BETS should reveal the types of sources responsible for the spectrum and the most reliable combination of diffusion parameters. Precise observations around 10 GeV will also enable us to analyze the details of solar-modulation effects and the reacceleration mechanism in the Galaxy.

The design of the PPB-BETS is basically the same as that for a BETS developed for lower latitude observations (Torii *et al.*, 2000). However, various improvements have been made (Torii *et al.*, 1999). The PPB-BETS instrument consists of a shower detector, which incorporates an imaging calorimeter and a trigger system, a data acquisition system and a telemetry system. The shower detector consists of multiple layers of scintillating fibers and lead plates. Incident high energy electrons induce a shower inside the multi-layer detector, which is observed as a three-dimensional characteristic pattern of light emissions. This optical image is intensified by a set of image intensifiers and recorded by a CCD camera system. Two sets of image-intensified CCD camera systems are used to simultaneously image the emission patterns on the X-Z and Y-Z planes, respectively; the three-dimensional pattern, where the Z-axis represents the vertical direction and the X-Y plane represents the horizontal plane, is then reconstructed. Figure 5, taken from Torii *et al.* (2000), shows an example of the images of the shower on the X-Z plane (panel (a)) and the Y-Z plane (panel (b)). All the data are processed electrically and transmitted via telemetry, hence the recovery of the instrument is not essential for data acquisition. This point is an important advantage for use in the PPB experiment because recovery in the Antarctic region is very difficult, especially for the PPB experiment. For example, an alternative observation technique that utilizes an emulsion chamber (*e.g.*, Nishimura *et al.*, 1997) can be used to observe spectrum up to a few TeV, but the instrument must be recovered in fact to obtain the observation data. The PPB-BETS has several other advantages over the emulsion chamber system, as discussed by Torii *et al.* (1999, 2000).

4. Geophysical observations

One of the main purposes of the geophysical observations that will be performed in the 2nd-PPB experiment is to observe various phenomena in the magnetospheric and ionospheric boundary layers. As shown in Fig. 2, the PPBs can traverse a large latitudinal range of magnetic coordinates and will float across several interesting regions and boundaries during their circumpolar trajectory. Figure 6 shows these regions and boundaries in the magnetosphere, and Fig. 7 shows the approximate locations of their ionospheric projection along the geomagnetic field lines. From lower latitudes, the PPBs can remain in the region of the plasma sphere, plasmapause, trough, auroral oval (plasma sheet), plasma sheet boundary layer (PSBL), low latitude boundary layer (LLBL), mantle region, cusp region, and polar cap (lobe) region. Small circles on the expected trajectory in Fig. 7 indicate the daily positions of the balloon. The PPBs are expected to remain for about 1–3 days in each region and boundary during their flight. We are planning to launch three balloons in as rapid succession as weather conditions permit (with an interval of less than 1 day) to place all three balloons in adjacent areas of the trajectory (separated by a few hundred kilometers) to form a cluster of balloons. Hence, the three balloons are referred to as a "Balloon Cluster", recalling the successful CLUSTER-2 satellite project in which four satellites were placed in the magnetosphere. The payload configurations of all three balloons are identical. Simultaneous observations with identical sets of instruments within and outside of the target regions and boundaries should enable the spatial distribution and temporal variations of various phenomena occurring around these regions and boundaries to be studied.

A list of the scientific objectives of the geophysical observations in the 2nd-PPB is shown in Table 4. Figure 8, taken from Fujii *et al.* (1994), shows the electromagnetic parameters across an area of intense auroral activity, westward traveling surge (WTS), observed by a low-altitude polar-orbiting satellite (DE-2). The satellite moved equator-

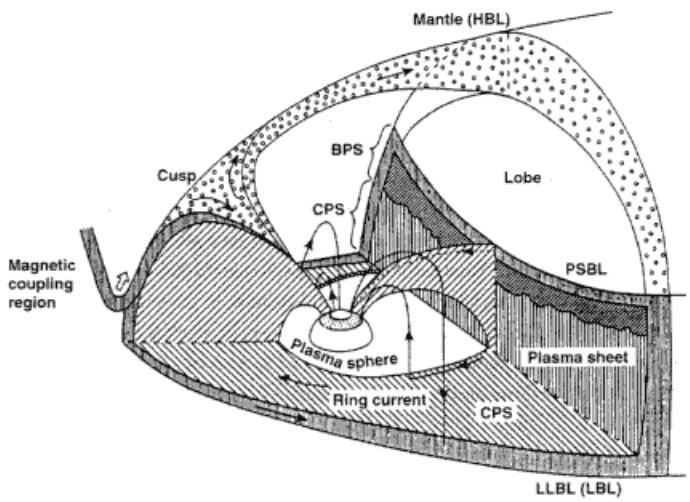

Fig. 6. Various regions and boundaries in the magnetosphere.

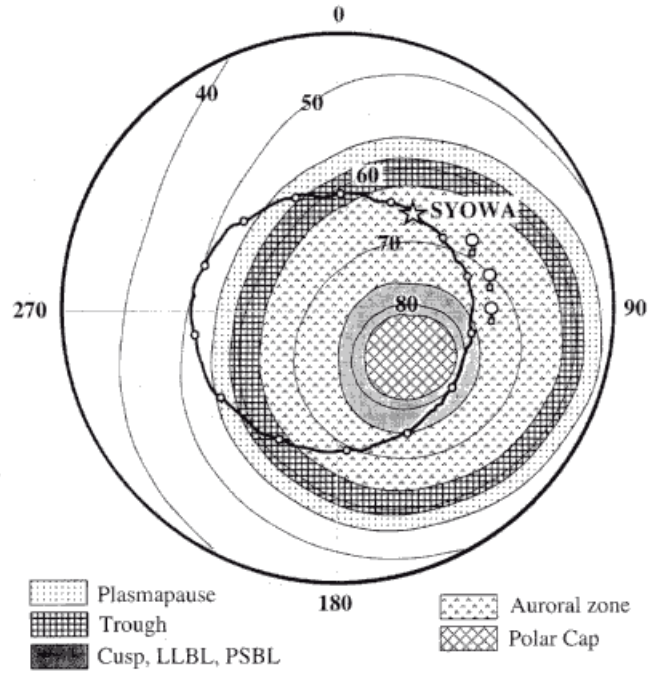

Fig. 7. Approximate location of the ionospheric projection of the various regions and boundaries in the magnetosphere. The expected trajectory of the PPB is also shown by the thick black line. The circles on the trajectory indicate the daily positions of the balloon.

Table 4. A list of scientific targets of geophysical observation in the 2nd-PPB campaign.

·Phenomena around the PSBL region, associated with substorm
·SAID (sub-auroral ion drift), associated with substorm
·Wave-particle interaction around the plasmapause
·Flux variation of the radiation belt particles, associated with storm
·Phenomena around the cusp, cleft, and mantle region, responding to variation in solar wind parameters
·Response of the polar cap convection to solar wind parameters
·Electromagnetic dynamics in the vicinity of auroral activity (*e.g.*, westward traveling surge, omega band)
·Local time dependence of the relationship among electric field, magnetic variation, and particle precipitation
·Source mechanism for the quasi-periodic VLF emission and particle precipitation in the Pc3 range
·Relationship between the ULF pulsation and auroral X-ray pulsation in the Pc5 range
·Quick response of electric field and magnetic variation at mid-latitude, to variation in the solar wind parameters
·Simultaneous observation of the Global Mode Pc5 with magnetospheric satellites and SuperDARN
·Variation in the atmospheric electric parameters, associated with solar events (*e.g.*, proton event)
·Relationship between the plasma flows observed by the SuperDARN and electric field and magnetic field vectors observed by PPB
·Relationship between the radar echo region observed by the SuperDARN and fluctuation of the total electron content and electric field observed by PPB

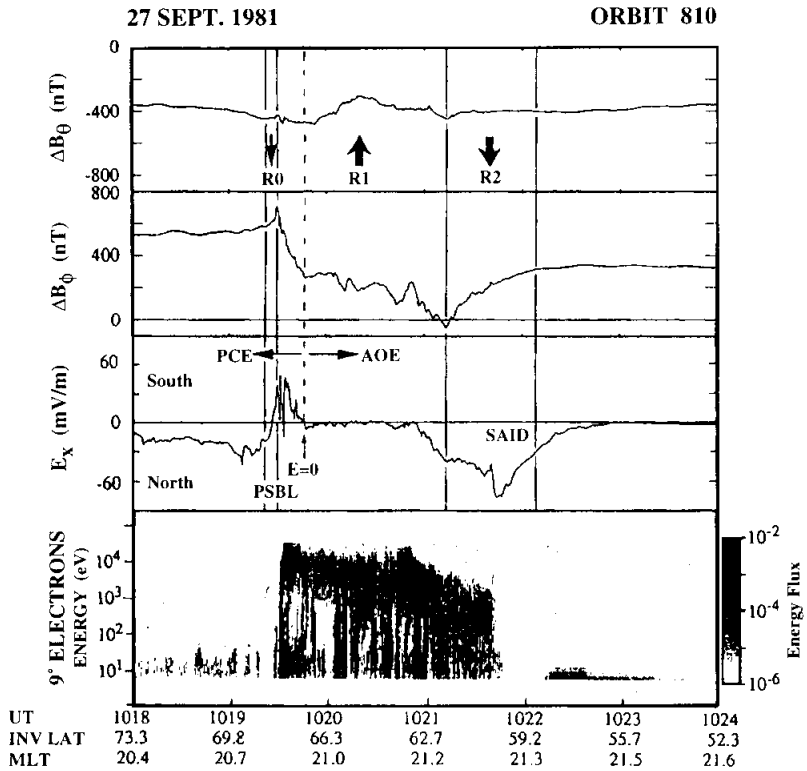

Fig. 8. Example observation of the PSBL region and SAID by the DE-2 satellite (after Fujii et al., 1994).

ward as time advanced from left to right in Fig. 8. Intense equatorward and poleward electric fields are visible around the poleward and equatorward boundaries of the auroral electron precipitation region, respectively. The former one is frequently observed in the PSBL region and is considered to be closely associated with the process around the X-type neutral line in the tail (*e.g.*, Burke *et al.*, 1994). A characteristic pattern of field-aligned currents (FAC), an intense hydromagnetic wave activity, and a velocity-dispersed ion precipitation structure (VDIS) are also observed around the PSBL region (*e.g.*, Fukunishi *et al.*, 1993; Wygant *et al.*, 2000).

The latter one around the equatorward boundary is called a "sub-auroral ion drift (SAID)" and is usually observed during the late expansion to recovery phase of a substorm predominantly in the pre-midnight, sub-auroral region around the trough region (*e.g.*, Spiro *et al.*, 1979; Anderson *et al.*, 1993; Karlsson *et al.*, 1998). These characteristics of the PSBL region and SAID have been mainly studied using low-altitude satellite observations. To our knowledge, very few observations of their temporal variations have been performed with a higher resolution than that of the satellite revolution period.

Auroral X-ray observations by PPB-6 in the 1st-PPB experiment revealed that the characteristic energy of auroral X-rays reaches a maximum value around the plasmapause region, as shown in Fig. 9 (Suzuki, 1996). Suzuki (1996) suggested that this result is due

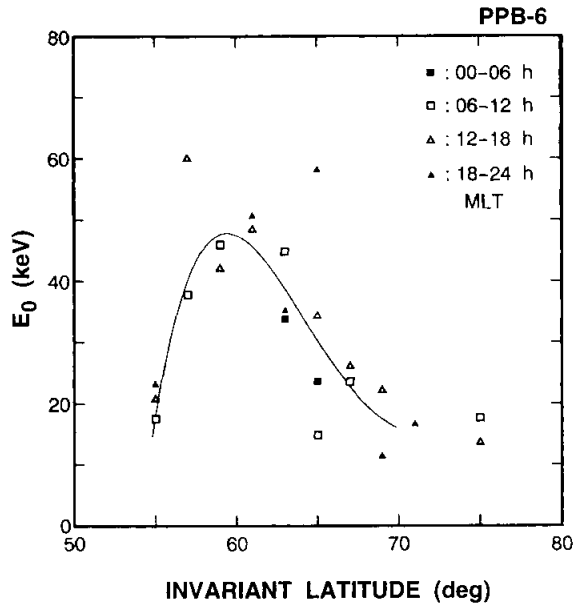

Fig. 9. Latitudinal distribution of the characteristic energies of auroral X-rays, observed by PPB-6 in the 1st-PPB experiment (after Suzuki, 1996).

to the characteristics of resonant electrons, which are scattered into the loss-cone by the electron-cyclotron resonance process with whistler mode waves. The location of the plasmapause is known to vary significantly in response to magnetospheric conditions (*e.g.*, Maynard and Chen, 1975). Observations using the "Balloon Cluster" in the 2nd-PPB experiment will enable us to investigate the spatial and temporal variations in wave-particle interactions around the plasmapause region.

The trajectory of the PPB runs across the regions of the outer belt and the slot region of the radiation belt around the southward edge of the South Atlantic Anomaly (SAA), as shown in Fig. 10a (Tsuruuchi, 1998). Energetic particle flux in the outer and inner belts and the slot region increases significantly during strong storm periods, as shown in Fig. 10b. The "Balloon Cluster" will enable the spatial distribution of energetic electron precipitation from the radiation belts and its temporal evolution during the development of a storm to be observed.

In the 2nd-PPB experiment, well-coordinated simultaneous observations with the SuperDARN HF-radar network, Antarctic stations, low-altitude satellites, NOAA, DMSP, AKEBONO, etc., and magnetospheric observations by CLUSTER-2, GEOTAIL, and geosynchronous satellites are also expected.

The EMW has three observational modes: 1) wave form observations in a frequency range of 0.2–4.0 Hz with 10-Hz sampling, 2) intensity observations for 4 specific frequency channels (300 Hz, 600 Hz, 1.2 kHz, and 2.4 kHz) with a 0.5-s resolution, and 3) frequency sweep observations at 4 specific frequencies (5 kHz, 10 kHz, 20 kHz, and 36 kHz) with a 0.5-s resolution. The EFD observes two horizontal and one vertical electric field components using a double spherical probe technique with resolutions of 0.2 mV/m (horizontal)

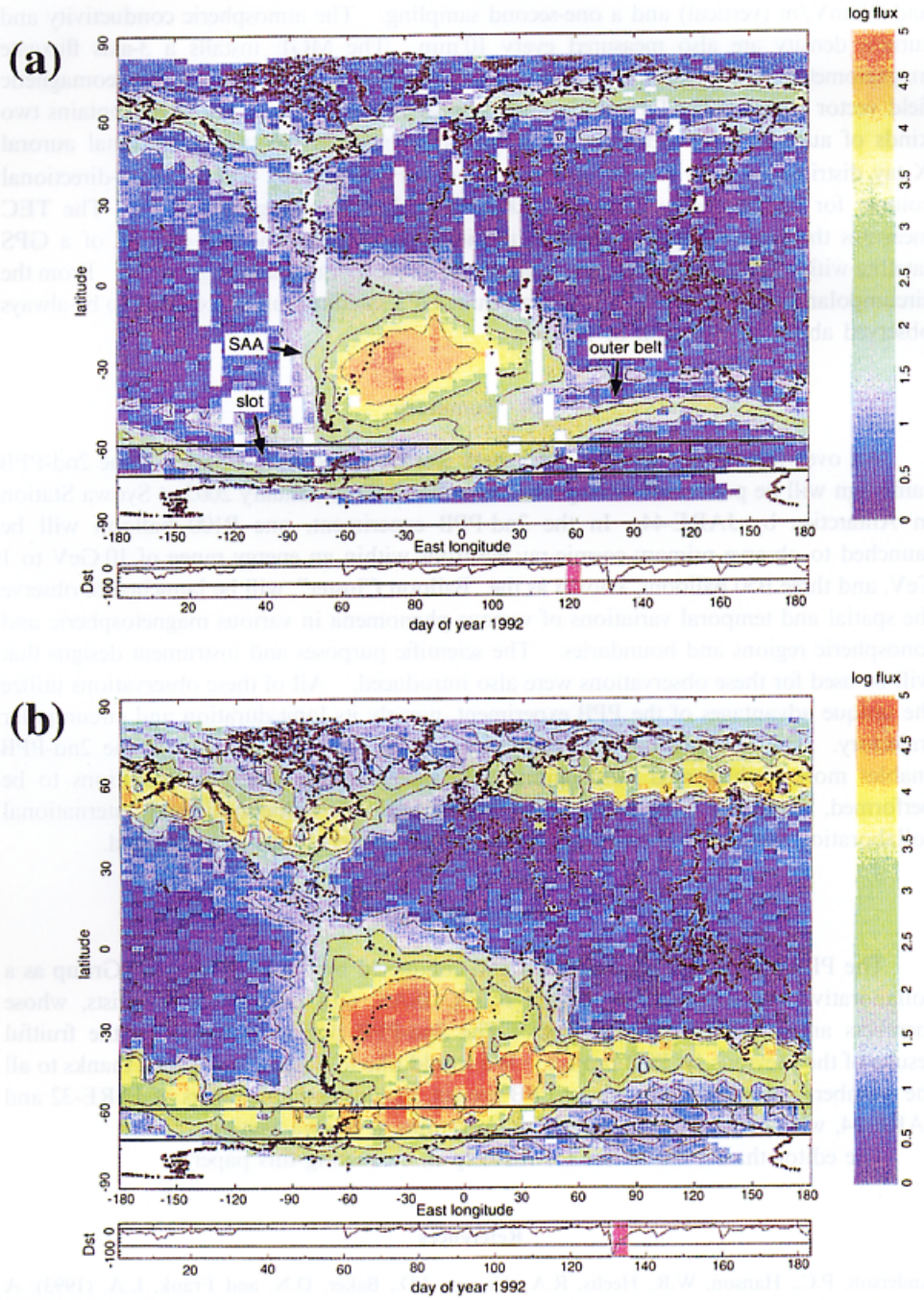

Fig. 10. Distribution of energetic electron (>300 keV) flux observed by the NOAA satellite during a quiet period (a) and a disturbed period (b) (after Tsuruuchi, 1998). The two horizontal black lines show the latitudinal range of the PPB trajectory.

and 0.8 mV/m (vertical) and a one-second sampling. The atmospheric conductivity and current density are also measured every 10 min. The MGF installs a 3-axis fluxgate magnetometer, 2-axis clinometer, and a set of sunsensors, and measures the geomagnetic field vector with a 0.25 nT resolution and one-second sampling. The AXI contains two kinds of auroral X-ray detectors: an imager that observes the two-dimensional auroral X-ray distribution with a 4×4 resolution and a FOV of 140°, and an omni-directional counter for higher energy X-rays (>200 keV) with a sampling rate of 1 s. The TEC measures the total electron content in the ionosphere along the line-of-sight of a GPS satellite with a GPS dual-frequency receiver and a one-minute sampling period. From the circumpolar trajectory of the PPB, at least three GPS satellites can be expected to be always observed above an elevation of 10°.

5. Summary

An overview of the 2nd-PPB experiment was described in this paper. The 2nd-PPB campaign will be performed during late December 2002 to January 2003 at Syowa Station in Antarctica by JARE-44. In the 2nd-PPB experiment, one B100 balloon will be launched to observe primary cosmic-ray electrons within an energy range of 10 GeV to 1 TeV, and three B50 balloons, known as the "Balloon Cluster", will be launched to observe the spatial and temporal variations of various phenomena in various magnetospheric and ionospheric regions and boundaries. The scientific purposes and instrument designs that will be used for these observations were also introduced. All of these observations utilize the unique advantages of the PPB experiment, namely its long duration and circumpolar trajectory. The new satellite data acquisition system that will be used in the 2nd-PPB enables more sophisticated observations with much higher temporal resolutions to be performed, compared with the 1st-PPB experiment. A well-coordinated international collaboration with ground-based and satellite-based observations is anticipated.

Acknowledgments

The PPB project has been planned and conducted by the PPB Working Group as a collaborative research program of the NIPR, ISAS, and nationwide scientists, whose members are gratefully acknowledged. The 2nd-PPB project is based on the fruitful results of the previous 1st-PPB project. We would like to express our special thanks to all the members participating in the 1st-PPB project, including the members of JARE-32 and JARE-34, who performed the launching operations at Syowa Station.

The editor thanks the referee for his help in evaluating this paper.

References

Anderson, P.C., Hanson, W.B., Heelis, R.A., Craven, J.D., Baker, D.N. and Frank, L.A. (1993): A proposed production model of rapid subauroral ion drifts and their relationship to substorm evolution. J. Geophys. Res., **98**, 6069–6078.

Burke, W.J., Machuzak, J.S., Maynard, N.C., Basinska, E.M., Erickson, G.M., Hoffman, R.A., Slavin, J.A. and Hanson, W.B. (1994): Auroral ionospheric signatures of the plasma sheet boundary

layer in the evening sector. J. Geophys. Res., **99**, 2489-2499.

Ebihara, Y., Kadokura, A., Tonegawa, Y., Tohyama, F., Sato, N., Hirasima, Y., Namiki, M., Bering, E.A., Benbrook, J.R. and Ejiri, M. (1996): A convection enhancement event observed with the Polar Patrol Balloon #4. Proc. NIPR Symp. Upper Atmos. Phys., **9**, 12-24.

Ejiri, M., Kadokura, A., Hirasawa, T., Sato, N., Fujii, R., Miyaoka, H., Nishimura, J., Yajima, N., Yamagami, T., Kokubun, S., Fukunishi, H., Yamanaka, M.D. and Kodama, M. (1993): Polar Patrol Balloon experiment in Antarctica. Adv. Space Res., **13**, 2, (2)127-(2)130.

Ejiri, M., Akiyama, H., Bering, E.A. Fujii, R., Hayashi, M., Hirasima, Y., Kadokura, A., Kanzawa, H., Kodama, M., Miyaoka, H., Murakami, H., Nakagawa, M., Namiki, M., Nishimura, J., Ohta, S., Suzuki, H., Tohyama, F., Tonegawa, Y., Yajima, N., Yamagami, T., Yamagishi, H. and Yamanaka, M.D. (1995): Experimental results of Polar Patrol Balloon project in Antarctica (extended abstract). Proc. NIPR Symp. Upper Atmos. Phys., **8**, 60-64.

Fujii, R., Miyaoka, H., Kadokura, A., Ono, T., Yamagishi, H., Sato, N., Ejiri, M., Hirasawa, T., Nishimura, J., Yajima, N., Yamagami, T., Ohta, S., Akiyama, H., Tsuruda, K., Kodama, M., Fukunishi, H., Yamanaka, M.D. and Kokubun, S. (1989): Polar Patrol Balloon experiment during 1991-1993. Nankyoku Shiryô (Antarct. Rec.), **33**, 320-328.

Fujii, R., Ono, K. and Ohta, S. (1992): Data transfer system using a multi-ID ARGOS transmitter for the antarctic Polar Patrol Balloon experiment. Nankyoku Shiryô (Antarct. Rec.), **36**, 350-362.

Fujii, R., Hoffman, R.A., Anderson, P.C., Craven, J.D., Sugiura, M., Frank, L.A. and Maynard, N.C. (1994): Electrodynamic parameters in the nighttime sector during auroral substorms. J. Geophys. Res., **99**, 6093-6112.

Fukunishi, H., Takahashi, Y., Nagatsuma, T., Mukai, T. and Machida, S. (1993): Latitudinal structures of nightside field-aligned currents and their relationships to the plasma sheet regions. J. Geophys. Res., **98**, 11235-11255.

Greenwald, R.A., Baker, K.B., Dudeney, J.R., Pinnock, M., Jones, T.B., Thomas, E.C., Villain, J.-P., Cerisier, J.-C., Senior, C., Hanuise, C., Hunsucker, R.D., Sofko, G., Koehler, J., Nielsen, E., Pellinen, R.A., Walker, D.M., Sato, N. and Yamagishi, H. (1995): DARN/SuperDARN: A global view of the dynamics of high-latitude convection. Space Sci. Rev., **71**, 761-796.

Hayashi, M., Murata, I., Fujii, R., Iwasaka, Y., Kondo, Y. and Kanzawa, H. (1994): Observation of ozone and aerosols in the Antarctic ozone hole of 1991 under the Polar Patrol Balloon (PPB) project -Preliminary result-. Ozone in the Troposphere and Stratosphere (Proc. Quadrennial Ozone Symp. 1992, Charlottesville, Virginia, U. S. A., June 4-13, 1992), ed. by R.D. Hudson. Houston, NASA (NASA Conf. Pub. 3266), 505-508.

Hirasima, Y., Shimobayashi, H., Yamagishi, H., Suzuki, H., Murakami, H., Yamada, A., Yamagami, T., Namiki, M. and Kodama, M. (1999): MHD wave characteristics inferred from correlations between X-rays, VLF, and ULFs at Syowa Station, Antarctica and Tjörnes, Iceland (L~6). Earth Planets Space, **51**, 33-41.

Kadokura, A., Ejiri, M., Ohta, S. and Akiyama, H. (1991): Polar Patrol Balloon (PPB) experiment of the 30th Japanese Antarctic Expedition (1989-1990). Nankyoku Shiryô (Antarct. Rec.), **35**, 143-154.

Kadokura, A. (1995): Numerical modeling of thermal behaviors and vertical motions of Polar Patrol Balloon with auto-ballasting system. J. Geomagn. Geoelectr., **47**, 377-404.

Kanzawa, H. and Kondo, Y. (1991): A plan for observation of the Antarctic ozone hole in 1991 under the Polar Patrol Balloon (PPB) project. Nankyoku Shiryô (Antarct. Rec.), **35**, 227-237.

Kanzawa, H., Fujii, R., Yamazaki, K. and Yamanaka, M.D. (1994): Trajectory analysis of Polar Patrol Balloon (PPB) flights in the stratosphere over Antarctica in summer and spring: A preliminary result. (Proc. Quadrennial Ozone Symp. 1992, Charlottesville, Virginia, U.S.A., June 4-13, 1992), ed. by R.D. Hudson. Houston, NASA (NASA Conf. Pub. 3266), 606-609.

Karlsson, T., Marklund, G.T. and Blomberg, L.G. (1998): Subauroral electric fields observed by the Freja satellite: A statistical study. J. Geophys. Res., **103**, 4327-4341.

Kodama, M., Suzuki, H., Hirasima, Y., Yamagami, T., Murakami, H. and Nishimura, J. (1995):

Circumpolar observation of bremsstrahlung X-rays by a Polar Patrol Balloon over Antarctica. J. Geomagn. Geoelectr., **47**, 253–266.

Maynard, N.C. and Chen, A.J. (1975): Isolated cold plasma regions: observations and their relation to possible production mechanisms. J. Geophys. Res., **80**, 1009–1013.

Nagata, T., Fukunishi, H., Nishimura, J., Kodama, M. and co-members of PPB working group. (1985): Polar Patrol Balloon project in Antarctica. Mem. Natl Inst. Polar Res., Spec. Issue, **38**, 156–163.

Nishimura, J., Kodama, M., Tsuruda, K., Fukunishi, H. and co-members of PPB working group. (1985): Feasibility studies of "Polar Patrol Balloon". Adv. Space Res., **5**, 87–90.

Nishimura, J., Yajima, N., Akiyama, H., Ejiri, M., Fujii, R. and Kokubun, S. (1994): Polar Patrol Balloon. J. Aircr., **31**, 1264–1267.

Nishimura, J., Kobayashi, T., Komori, Y. and Yoshida, K. (1997): Observations of high energy primary electrons and their astrophysical significance. Adv. Space Res., **19**, 767–770.

Spiro, R.W., Heelis, R.A. and Hanson, W.B. (1979): Rapid subauroral ion drifts observed by Atmosphere Explorer C. Geophys. Res. Lett., **6**, 657–660.

Suzuki, H. (1996): Broad-spatial characteristics and energy spectrum characteristics of auroral X-rays observed by a Polar Patrol Balloon. Nankyoku Shiryô (Antarct. Rec.), **40**, 125–155.

Tohyama, F., Fujii, R. Ejiri, M. and Yajima, N. (1993): Observations of the geomagnetic field by Polar Patrol Balloon (PPB) experiment in Antarctica. Proc. NIPR Symp. Upper Atmos. Phys., **6**, 15–24.

Torii, S., Yamagami, T., Yuda, T. and Kasahara, K. (1999): Measurement of high-energy cosmic-ray electrons with a Polar Patrol Balloon. Adv. Polar Upper Atmos. Res., **13**, 176–181.

Torii, S., Tamura, T., Tateyama, N., Yoshida, K., Ouchi, T., Yamagami, T., Saito, Y., Murakami, H., Kobayashi, T., Komori, Y., Kasahara, K., Yuda T. and Nishimura, J. (2000): The balloon-borne electron telescope with scintillating fibers (BETS). Nucl. Instr. Meth., **A 452**, 81–93.

Tsuruuchi, A. (1998): Studies on variation of the radiation belt particle at South Atlantic Anomaly, Master thesis, Tohoku Univ., Sendai, Japan.

Wygant, J.R., Keiling, A., Cattell, C.A., Johnson, M., Lysak, R.L., Temerin, M., Mozer, F.S., Kletzing, C.A., Scudder, J.D., Peterson, W., Russell, C.T., Parks, G., Brittnacher, M., Germany, G. and Spann, J. (2000): Polar spacecraft based comparisons of intense electric fields and Poynting flux near and within the plasma sheet-tail lobe boundary to UVI images: An energy source for the aurora. J. Geophys. Res., **105**, 18675–18692.

Yamagami, T., Namiki, M., Ohta, S., Yajima, N., Suzuki, H., Hirasima, Y., Murakami, H., Morimoto, K., Yamagiwa, I., Nakagawa, M., Takahashi, T., Murakami, S., Nishimura, J., Tonegawa, Y., Ejiri, M., Sato, N., Kohno, T. and Kodama, M. (1994): A Polar Patrol Balloon observation of cosmic-ray protons and auroral X-rays in Antarctica. J. Geomagn. Geoelectr., **46**, 903–908.

Yamanaka, M.D., Yamazaki, K. and Kanzawa, H. (1988): Studies of middle atmosphere dynamics under the Polar Patrol Balloon (PPB) project: Present status and future plans. Proc. NIPR Symp. Upper Atmos. Phys., **1**, 65–74.

(Received February 1, 2002; Revised manuscript accepted April 23, 2002)